Journal of Power Sources 194 (2009) 328–337

Contents lists available at ScienceDirect

Journal of Power Sources

journal homepage: www.elsevier.com/locate/jpowsour

Uneven gas diffusion layer intrusion in gas channel arrays of proton exchange membrane fuel cell and its effects on flow distribution

S.G. Kandlikar*, Z. Lu, T.Y. Lin, D. Cooke, M. Daino

Thermal Analysis, Microfluidics, and Fuel Cell Laboratory, Rochester Institute of Technology, 76 Lomb Memorial Dr., Rochester, NY 14623, United States

ARTICLE INFO

Article history:
Received 11 March 2009
Received in revised form 1 May 2009
Accepted 5 May 2009
Available online 22 May 2009

Keywords:
PEMFC
Gas channels
Gas diffusion layer
Intrusion
Flow maldistribution
GDL heterogeneity

ABSTRACT

Intrusion of the gas diffusion layer (GDL) into gas channels due to fuel cell compression has a major impact on the gas flow distribution, fuel cell performance and durability. In this work, the effect of compression resulting in GDL intrusion in individual parallel PEMFC channels is investigated. The intrusion is determined using two methods: an optical measurement in both the in-plane and through-plane directions of GDL, as well as an analytical fluid flow model based on individual channel flow rate measurements. The intrusion measurements and estimates obtained from these methods agree well with each other. An uneven distribution of GDL intrusion into individual parallel channels is observed. A non-uniform compression force distribution derived from the clamping bolts causes a higher intrusion in the end channels. The heterogeneous GDL structure and physical properties may also contribute to the uneven GDL intrusion. As a result of uneven intrusion distribution, severe flow maldistribution and increased pressure drop have been observed. The intrusion data can be further used to determine the mechanical properties of GDL materials. Using the finite element analysis software program ANSYS, the Young's modulus of the GDL from these measurements is estimated to be 30.9 MPa.

1. Introduction

Among the components of the membrane electrode assemblies (MEAs) of proton exchange membrane fuel cells (PEMFCs), much effort has been devoted to the development of membranes [1,2] and electro-catalysts [3,4]. Until recently, very little attention has been paid to the gas diffusion layer (GDL) despite its important role in fuel cell operation. The primary functions of a GDL are to supply reactant gases and remove product water from the catalyst layers, to conduct electricity and heat between adjacent components, and to provide mechanical support for the MEA. These functions impose stringent requirements on the electrical, transport, and mechanical properties of the GDL. The most commonly used GDLs are carbon-fiber-based paper or cloth. These materials are highly porous, having a porosity of about 80% at free standing state, to provide efficient passageways for water and gases. In order to improve the water management of a PEMFC, these fibrous materials are usually wet-proofed with polytetrafluoroethylene (PTFE) [5]. A fine microporous layer (MPL), which mainly consists of carbon powder and PTFE particles, is often coated on one side of the GDL near the catalyst layer to improve the fuel cell performance [6,7]. It is generally believed that the MPL coating improves the cell performance through one or a combination of the following mechanisms: (a) increasing effective drainage of water from the catalyst layer-GDL interface by the capillary forces due to the presence of two different pore sizes [8]; (b) improving the humidification of the membrane at the anode side [6,9]; (c) increasing oxygen diffusion by reducing flooding in the cathode [9,10]; (d) enhancing the formation and transport of the water vapor in the CL and MPL [11]; (e) improving the electrical contact between GDL and catalyst layers [6].

In a fuel cell stack, the cell components are assembled together under a compressive load to prevent gas leakage and to reduce the contact resistance between the GDL and the bipolar plate. However, over-compression of the GDL leads to poor cell performance. Many researchers have studied the effect of compressive stresses on fuel cell performance. Lee et al. [12] studied the influence of compression on PEMFC performance with different types of GDLs and found that the performance was a function of the compression pressure and GDL materials. Ge et al. [13] and Escribano et al. [14] also studied the effect of GDL compression on PEMFC performance. Both of their results showed that the fuel cell performance at high current densities decreased with the increase in compression force. Zhou and Wu [15] numerically simulated the effect of the GDL compression deformation on the performance of PEMFCs.

Abbreviations: CL, catalyst layer; GDL, gas diffusion layer; MEA, membrane electrode assembly; MPL, microporous layer; PEM, proton exchange membrane; PEMFC, proton exchange membrane fuel cell; PTFE, polytetrafluoroethylene.

* Corresponding author. Tel.: +1 585 475 6728; fax: +1 585 475 7710.
E-mail address: sgkeme@rit.edu (S.G. Kandlikar).

0378-7753/$ – see front matter © 2009 Elsevier B.V. All rights reserved.
doi:10.1016/j.jpowsour.2009.05.019

Nomenclature

Symbols

A_c	cross-sectional area of a gas channel (m^2)
D_h	hydraulic diameter of the gas channel (m)
f_{app}	apparent friction factor, dimensionless
H	channel height (m)
P_w	wetted perimeter (m)
Δp	pressure drop across the gas channel (Pa)
Δp_{core}	friction pressure drop (Pa)
$\Delta p_{GDL,core}$	friction pressure drop with GDL (Pa)
$\Delta p_{GDL,meas}$	measured pressure drop in the channel with GDL (Pa)
Δp_{minor}	minor pressure drop (Pa)
$\Delta p_{plast,core}$	friction pressure drop with a plastic sheet (Pa)
$\Delta p_{plast,meas}$	measured pressure drop with a plastic sheet (Pa)
$Q_{mod,ch(n)}$	modified flow rate for channel n ($m^3\ s^{-1}$)
$Q_{est,ch(n)}$	flow rate of channel n determined from pressure drop data ($m^3\ s^{-1}$)
Q_{meas}	measured total flow rate from flow meter ($m^3\ s^{-1}$)
Re	Reynolds number (dimensionless)
u	velocity ($m\ s^{-1}$)
W	channel width (m)
x	length (m)
x^+	developing length (dimensionless)

Greek letters

α_c	aspect ratio (dimensionless)
μ	viscosity ($N\ s\ m^{-2}$)

Their results show that the fuel cell performance decreases with increasing compression. The performance loss caused by the compression was primarily ascribed to the increase in mass transport loss due to the reduction of GDL porosity and gas permeability. A GDL has a characteristically soft and brittle structure, which readily leads to deformation or damage when compressed. As a consequence, the microstructure and the physical properties of the GDL, e.g., porosity, diffusivity, electrical conductivity, etc., are considerably changed under compression. Nitta et al. [16,17] investigated the effects of compression (in terms of compressed GDL thickness) on gas permeability, in-plane and through-plane electric conductivities, and contact resistances at the interfaces. They found that the compression of GDL reduces gas permeability and contact resistance, while improving bulk conductivity. Feser et al. [18] measured the GDL in-plane permeability under various compressions and found an approximate linear decrease of in-plane permeability with compression. The influence of compressing a GDL on liquid water transport behavior as well as on the GDL microstructure morphology was studied by Bazylak et al. [19]. The compression of the GDL was found to cause fibers to breakup and deteriorate the hydrophobic coating which contributes to the formation of preferential pathways for liquid water transport in the GDL.

It is particularly worth noting that most papers on fuel cell compression and its effect on PEMFC performance considered a homogeneous GDL compression. In reality, the deformation of the GDL in a PEMFC is not homogeneous due to the flow field structure. The parts of the GDL under the lands of the flow field plate are significantly more compressed than the parts under the channel. This phenomenon has not received much attention until recently. Hottinen and Himanen [20] and Hottinen et al. [21] numerically investigated the effect of inhomogeneous compression of GDL on the temperature distribution and mass and charge transfer in a PEMFC. They concluded that the inhomogeneous compression causes a variety of contact resistances between the GDL and electrodes, resulting in significant effects on the temperature and current density distribution. The inhomogeneous problem is compounded by GDL intrusion into the channels. The high compression pressure pushes the softer GDL material into the channel, partially blocking the gas flow. GDL intrusion may lead to significant local variations of mass (both gas reactants and product water) transport in the channels and GDL. Nitta et al. [16] and Lai et al. [22] experimentally determined the GDL intrusion by using a floating bar technique. It was found that the GDL is compressed very little under the channel whereas GDL under the land is compressed to gasket thickness. Lai et al. [22] further modeled the channel intrusion of GDL and the flow redistribution in parallel channels. Their results suggested that a 5% variation in GDL intrusion could result in a 20% reduction of reactant flow in the most intruded channel. Basu et al. [23] developed a complete PEMFC two-phase flow model which included two-phase flow in both anode and cathode channels. The specific effect of GDL intrusion in the edge channels on channel flooding was studied numerically. Severe flow and liquid water maldistributions were found in the intruded channels due to the increased flow resistance. GDL intrusion reduced flow through the intruded channel, making it more difficult to flush liquid water out of the channel. They also pointed out that innovative flow field designs are needed to mitigate flow maldistribution and the ensuing adverse impact on cell performance and durability.

Even though GDL intrusion was determined in a few studies [16,22], only a simple case with a single channel has been studied in the literature. A real PEMFC usually implements a large active area and contains a large number of parallel channels. The local compression force derived from the location distribution of the clamping bolts is expectedly non-uniform. This may cause local variations in GDL intrusion. This problem is further compounded by the heterogeneity in the GDL microstructure and physical properties which may cause non-uniform GDL intrusion. Such an inhomogeneous GDL intrusion was already assumed in the modeling [23], but experimental verification is still missing.

This work focuses on the experimental measurement of the GDL intrusion in parallel gas channels and its effect on the flow distribution. For this purpose, an *ex situ* setup has been built, which allowed for the measurement of the instantaneous flow rate in individual channels and the determination of GDL intrusion. GDL intrusion in parallel channels has been measured with a confocal microscope in the in-plane and through-plane directions of the GDL. Flow distribution in each parallel channel has been measured at different compressions. The reduction in channel cross-sectional area is determined from the individual flow rates and compared to optical measurements. Based on these intrusion measurements, the elastic modulus for the GDL is estimated by using a finite element (ANSYS) model.

2. Experimental

2.1. Gas channels and GDL material

In order to simulate the real situation in a PEMFC, the gas channels were adopted from an actual fuel cell flow field design [24,25]. Eight parallel channels, each 183 mm long, 0.7 mm wide, and 0.4 mm deep with a land width of 0.5 mm between adjacent channels, were fabricated in a polycarbonate plate (Lexan®). These channels, if used in a fuel cell, would give an active area of 18.2 cm^2.

The GDL materials used in this work were provided by General Motors. In order to improve the water management performance, the GDL was PTFE treated and coated with an MPL. The GDL had a thickness of approximately 230 μm. A hard-stop PTFE gasket with a proper thickness was used to mimic the compression situation in the real fuel cell.

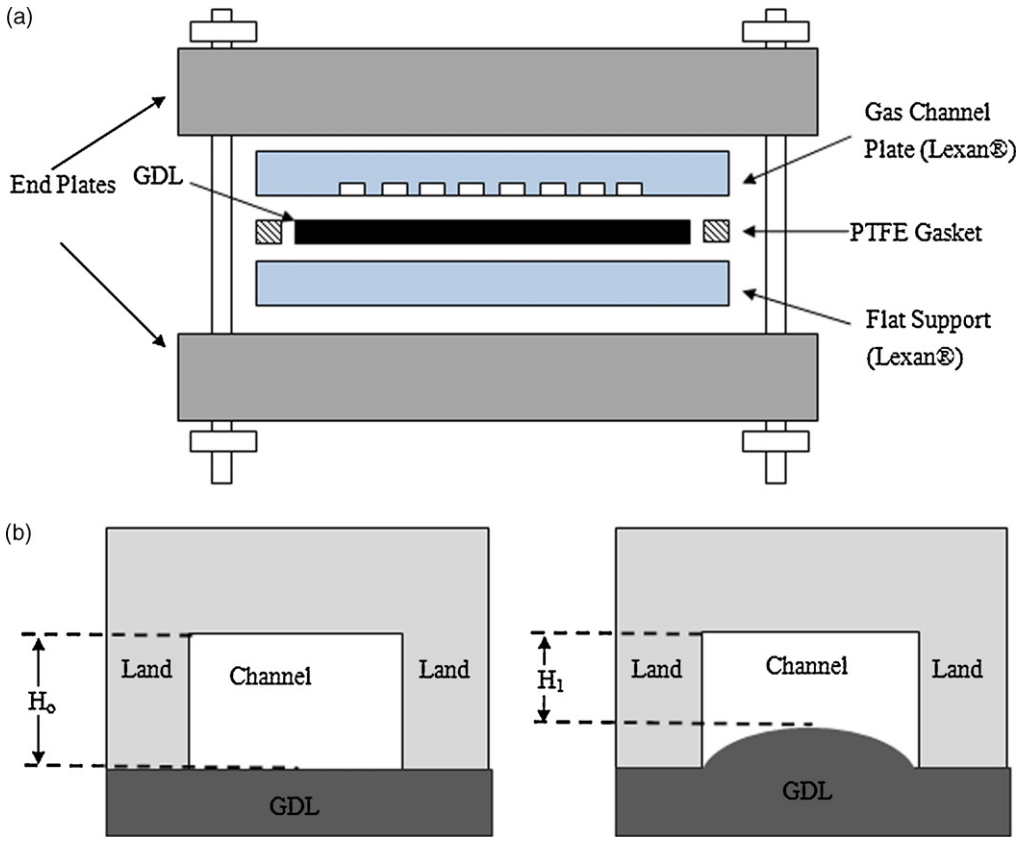

Fig. 1. Schematic of cross-sectional intrusion measurement method: (a) test fixture and (b) intrusion measurement.

2.2. Optical measurements

A confocal digital microscope (Keyence VHX-500) was used to measure the GDL intrusion in two directions. For one direction, the measurement was taken at the cross-section of the GDL. To do this, a section of the gas channels was cut, and the GDL was sandwiched between the gas channel plate and a flat support (Lexan®). The assembly was then inserted in-between two metal endplates and compressed by the bolts. The torch of each bolt was controlled and used to estimate the compression stress. A U-shaped PTFE gasket (one side open for the visual access) was used to mimic the compression conditions in a fuel cell. The GDL edge was recessed from the edge of the channel and the support plate to ensure appropriate compression. Fig. 1(a) shows the test fixture used to measure the cross-sectional GDL intrusion that results from cell compression. Fig. 1(b) illustrates the measurement process. The distance between the top surface of the GDL and the top of the channel was measured with Keyence software and used to calculate the GDL intrusion into the channels. This distance, with value H_0 at non-compression state, was reduced to H_1 upon compression. The intrusion was calculated as $H_0 - H_1$ for the applied compression. The compression in the range of 0–10 MPa was tested. The GDL intrusion for decreasing compression was also measured.

The intrusion was also measured at the central section of the entire channels in a test section shown in Fig. 2(a). A small pocket was milled into the Lexan channel plate and eight through holes of 0.7 mm diameter each were drilled for the visual access to the GDL in each gas channel. The depth between the uppermost fibers of the GDL and a reference surface (which for these measurements was the bottom of the small pocket milled into the test section) was measured using the Keyence VHX-500 system. Before the experiments, the exact depth of each hole (used as reference height) was calibrated by using a flat piece of plastic in place of the GDL. The GDL intrusion in each channel was then found from the difference between the reference height without GDL and the measured distance from the top of the GDL surface to the top of the hole. Fig. 2(b) shows the test section assembly, along with the springs which provide the compression. The water plate in Fig. 2(b) was used to introduce water to the test section to simulate an operating fuel cell. However, in this work no water was applied. The test section was compressed to different compressions in the range of 0.7–2.07 MPa and the intrusion was determined.

2.3. Flow measurements

Since GDL intrusion reduces the hydraulic diameter of reactant gas channels, a direct effect of channel intrusion can be seen as an increase of the reactant gas pressure drop from the inlet to the outlet of the flow field. Flow through an intruded channel is thus reduced under a given total pressure drop, leading to a flow maldistribution. An instantaneous flow rate measurement method based on the pressure drop measurement in individual channels at the entrance region has been developed in the authors' laboratory [25,26]. This technique measures the pressure drop over a small distance in the entrance region of the channel and is then converted to the flow rate in each individual channel. The pressure drop measurements can also provide an estimate of channel intrusion once the flow rates are known in each channel.

The test section used for the flow measurement was similar to the one in Fig. 2 except that no pockets were milled on the channel plate. The GDL was sandwiched between the air channel and the water channel designed to simulate a real PEMFC. In this portion of the study, the main objective was to measure the flow rates through an individual channel at different compressions and there-

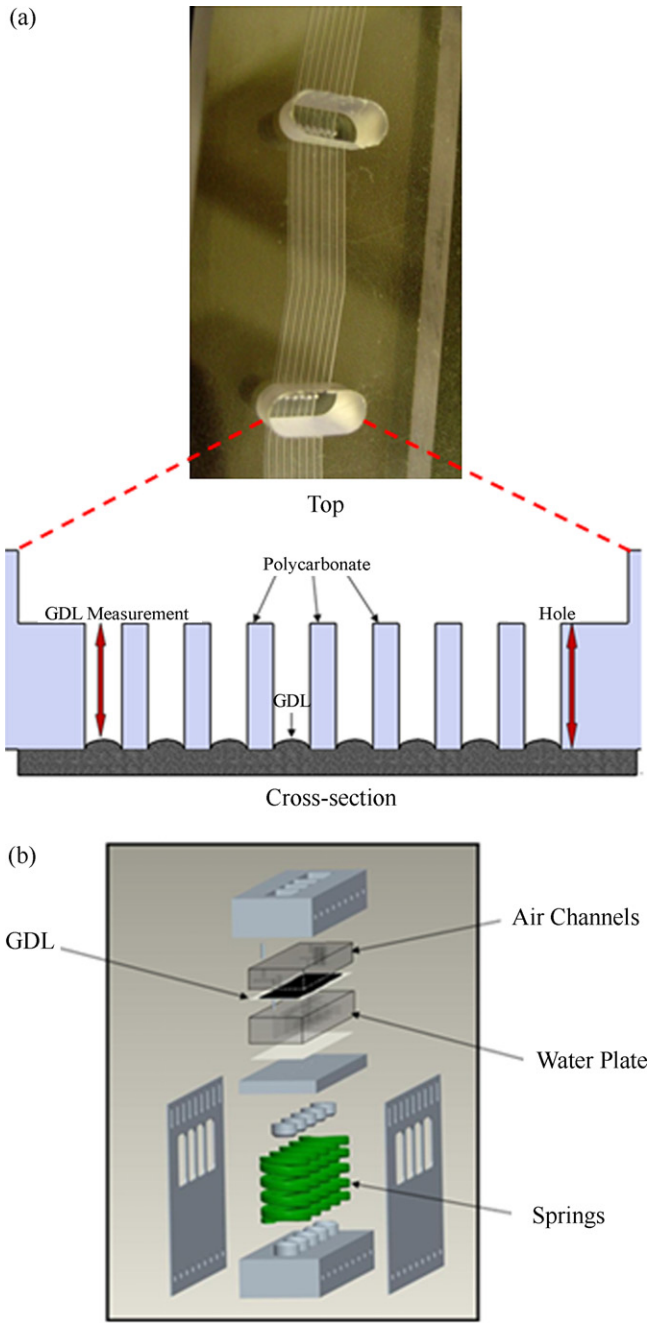

Fig. 2. (a) Central intrusion optical method and (b) test section assembly view for central intrusion method and fluid mechanics model.

fore no water was flowing through the water channels. The header was specially designed to allow the measurement of the pressure drop in the entrance region [25,26]. Dry air from a zero-grade air generator was used as the working fluid and the total input flow rate was measured before being introduced in the test section. The pressure drops in each channel were measured with differential pressure sensors (Honeywell FP2000) and recorded using a LabVIEW program. The total pressure difference between the inlet and outlet headers was also measured by a pressure transducer. The total input air flow rates were varied in the range of 0–5000 sccm. The test section was compressed with a Tinius Olsen compression machine and the compressive pressures were varied in the range of 0.7–2.07 MPa.

2.4. Finite element (ANSYS) modeling

Although it is possible to numerically calculate the GDL intrusion, e.g., from a finite element model [22], it has not been attempted in this work because this requires a complete characterization of the mechanical properties (e.g., stress–strain behavior, in-plane and through-plane elastic modulus, shear modulus, etc.) of GDL, which are not readily available. In addition, most of the previous characterization of the mechanical properties were made on GDLs without a MPL [5,22], whereas an MPL coating was attached to the carbon fiber for the GDL used in this work. It should be noted that the diffusion layer in a PEMFC generally contains an MPL to improve its water management performance. Therefore, our main interest in this modeling portion of the study was to obtain an estimation of the elastic modulus using the ANSYS modeling based on the measured intrusion values.

A finite element analysis (ANSYS) program was used to model the GDL intrusion. In order to simplify the calculation, the GDL was modeled as a linearly elastic, isotropic material. In the preprocessor solver, a solid 8 node 183 element type was selected to simulate modeling one channel and two lands. A mesh size of 0.02 mm was selected to create the elements, which was further refined at the upper and lower regions of the GDL interfaces. This mesh was validated by varying the mesh size in a range from 50% to 200% of the mesh size employed. The intrusion height varied only by less than 1.5%, which indicated that the 0.02 mm mesh size was appropriate. A boundary condition was applied to the bottom GDL surface (which sits on a solid flat support), constraining all degrees of freedom to zero for no displacement. The upper channel plate was loaded for an applied pressure in the range of 0.7–2.07 MPa. After the loading was applied, the model was solved for a contour plot of the displacement due to compression.

ANSYS needs initial input values for Young's modulus and Poisson's ratio for the material. Little information is available for the mechanical properties of carbon fiber paper, or even more specifically commercial GDLs which are PTFE treated and MPL coated. The Young's Modulus has been estimated only for Toray carbon paper in open literature. As an initial estimate, the modulus for Toray paper (TGP-H-060) of 17.9 MPa, which was obtained from the compression curve in the compression range of 0–2.75 MPa [5], was used. Since the GDL has a very high open porous structure (porosity of around 80%), Poisson's ratio was assumed to be zero.

3. Results and discussion

3.1. GDL intrusion from optical measurement

The GDL intrusion is defined as the vertical distance from the apex of GDL surface facing the reactant gas channel to the plane of the lands. The intrusion is first measured with a confocal microscope from the cross-section of GDL and gas channels. Fig. 3 shows the view of the deformed GDL in channel 3 at different compressions, as a typical example. The dotted rectangular shape in each image represents the air channel. The burrs in the channel formed from cutting, seen in Fig. 3, have not been cleared as they do not affect the measurements due to the fact that the GDL is recessed from the edge of the channel. The region under the GDL has been carefully cleared of the burrs. The GDL has a uniform thickness in a non-compressed state and the thickness decreases upon compression, as expected. Under compression, the shape of the GDL is deformed and part of it intrudes into the gas channel, partially blocking the channels.

Fig. 4 shows the intrusion data measured in selected channels (channel 1, 3, 5 and 7) as a function of compression and Table 1 lists the complete measurements. The GDL intrusion increases with

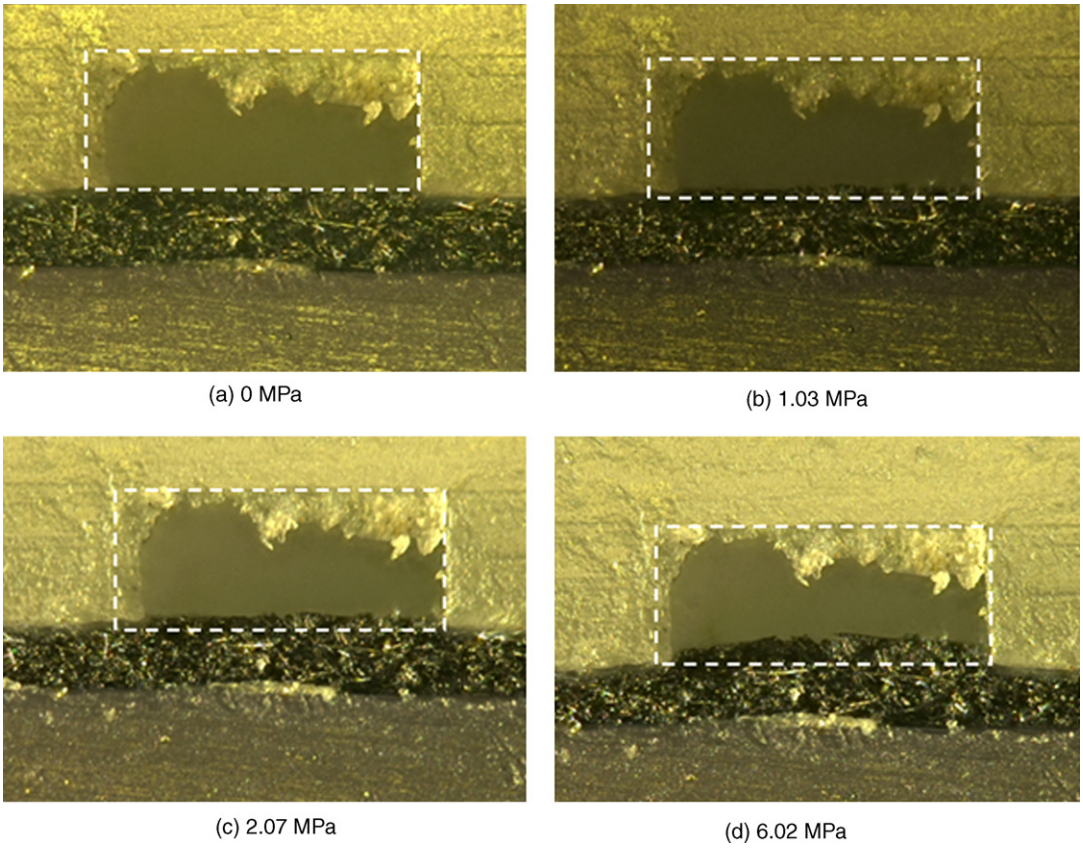

Fig. 3. Images of GDL intrusion in channel 3 at different compressions. The dotted rectangular outline in each image represents the air channel. The burrs seen on the channels have been removed from the land region.

Table 1
The measured intrusion into channel (in μm).

Compression	1.03 MPa	2.07 MPa	4.14 MPa	6.20 MPa	8.27 MPa	10.34 MPa
Channel 1	7.9 ± 3.2	39.1 ± 0.9	61.1 ± 1.6	78.9 ± 1.5	95.6 ± 0.9	111.0 ± 1.6
Channel 2	8.4 ± 3.2	34.0 ± 0.8	49.9 ± 0.8	68.3 ± 0.96	83.0 ± 1.2	96.5 ± 1.0
Channel 3	5.3 ± 2.2	39.9 ± 1.7	50.0 ± 2.6	70.8 ± 2.8	84.1 ± 1.5	100.3 ± 1.5
Channel 4	2.5 ± 1.8	23.7 ± 1.1	37.5 ± 0.9	54.7 ± 0.5	66.6 ± 1.1	77.3 ± 1.2
Channel 5	0.2 ± 1.3	21.7 ± 1.3	39.6 ± 1.8	52.0 ± 1.7	61.4 ± 1.6	74.2 ± 1.1
Channel 6	0.4 ± 1.6	25.8 ± 1.6	34.2 ± 1.0	50.4 ± 0.4	65.5 ± 2.0	78.8 ± 3.2
Channel 7	1.2 ± 3.0	32.3 ± 0.8	47.7 ± 0.4	62.7 ± 1.06	78.2 ± 1.1	92.2 ± 2.0
Channel 8	3.6 ± 2.6	36.9 ± 0.3	59.4 ± 2.3	73.1 ± 3.5	90.0 ± 2.1	103.7 ± 1.6

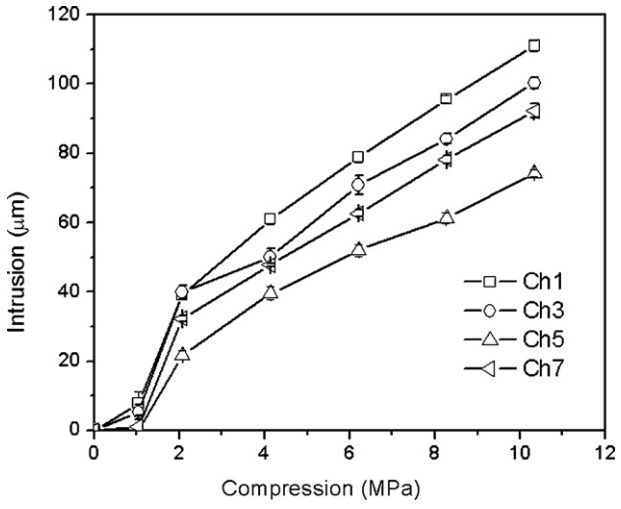

Fig. 4. GDL intrusion in selected channels 1, 3, 5, and 7 as a function of compression.

increasing compression, leading to a reduced hydraulic diameter of the channel. A more important finding from Fig. 4 is that the GDL intrusion is not uniform; rather it varies from channel to channel. A clearer demonstration of this behavior is shown in Fig. 5, in which the intrusions at a compression of 2.07 MPa in all eight channels are compared. Higher intrusion is observed in the edge channels, for example, channels 1, 7 and 8. This may be a result of the higher compression pressure caused by the location of bolts at the edges of the test fixture.

Fig. 6 shows the GDL intrusion in channel 3 during an increasing and then decreasing compression loading. A hysteresis is clearly observed, yielding a much higher intrusion during the decreasing compression loading. The results indicate that the GDL is not able to recover completely after intrusion. This is due to the permanent deformation or damage caused during the increasing loading. The same behavior is also observed in other channels. Similar hysteresis of GDL intrusion during increasing and decreasing compression was also reported in literature [5,27].

In order to validate the intrusion measurements from the cross-section of a GDL, which may contain damage due to die-cutting,

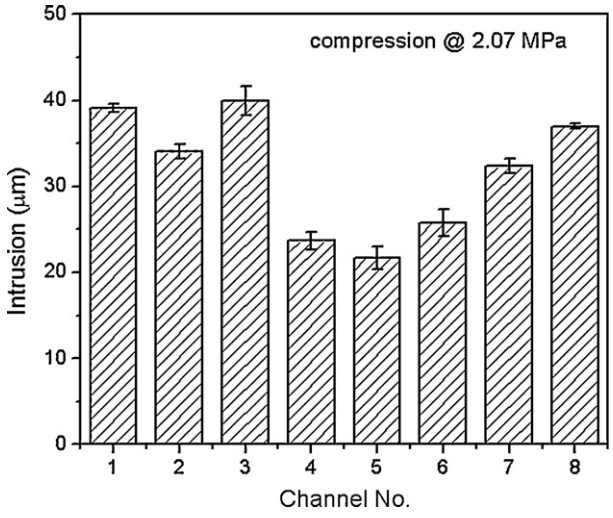

Fig. 5. GDL intrusion in individual channels at compression of 2.07 MPa.

measurements have also been conducted at the central section of the gas channels. The distance from the uppermost surface of the GDL to the channel top is measured with the confocal microscope. The measurements are carried out in three distinct locations over the entire channel length (183 mm) and the average intrusion is determined for each channel. Fig. 7(a) shows an image of the GDL top surface at a magnification of 300×. It should be pointed out that due to the difficulty in focusing on the highest point on an upper fiber, some uncertainty exists for the intrusion data. The magnitude of this uncertainty could be as large as one fiber diameter (approximately 8 μm). Fig. 7(b) shows a height contour of the GDL surface observed through one of the visual access holes.

The GDL intrusions measured in the central section of each channel at different compressions are summarized in Table 2. By comparing with Table 1, the intrusion heights measured from the central section of the channels agree well with those from the cross-sectional measurements at higher compression (e.g., at 2.07 MPa), but deviate at lower compression. Fig. 8 shows the average GDL intrusion measured at the central section of each gas channel at the compression of 2.07 MPa, as a typical example. An intrusion in the range of 20–40 μm is obtained, which is comparable to the measurement from the GDL cross-section (see Fig. 5). This result validates the more accurate measurement from the cross-section

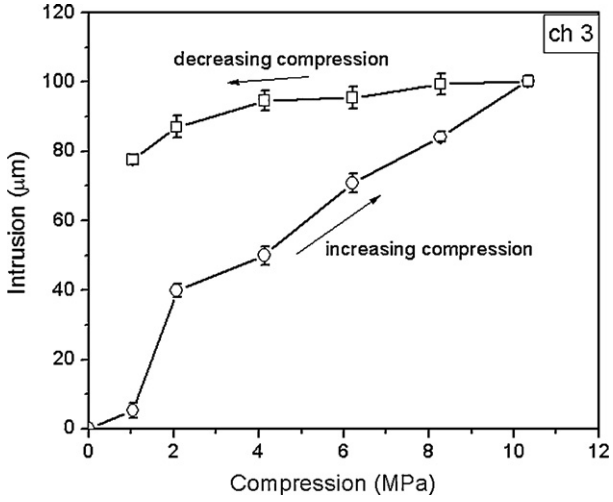

Fig. 6. The GDL intrusion in channel 3 with increasing and decreasing compression showing a hysteresis effect.

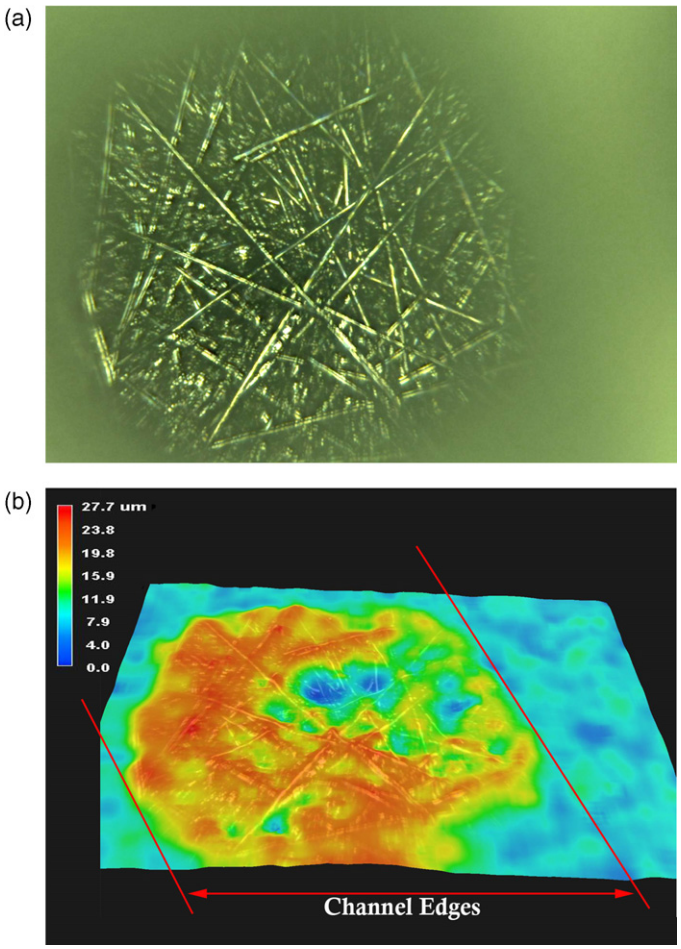

Fig. 7. (a) Image of GDL top surface at a magnification of 300× and (b) 3D contour image of GDL surface at a magnification of 300×.

of the GDL. An uneven distribution of intrusion is again clearly observed from Fig. 8. The channels at the edges, e.g., channel 1 and channel 8, display higher intrusion than the central channels. A similar trend has been observed based on the GDL cross-sectional measurement (Fig. 5).

The uneven GDL intrusion may be caused by the local variation of compression and/or the GDL material. A higher compression pressure is generally obtained for the channels near the edges, which is close to the location of the tightening bolts. This can account for the higher intrusions in the channel 1 and channel 8 in Figs. 5 and 8, respectively. However, a comparable intrusion is also observed in some other channels, for example, channel 3 in Fig. 5 and channels 5 and 7 in Fig. 8. These results cannot be explained by only the variation of the compression pressure. The GDL material itself may contribute to the uneven distribution of intrusion as well. Carbon fiber based GDL is a highly heterogeneous material, having a signif-

Table 2
GDL intrusion measured in central channels (in μm).

Compression	0.7 MPa	1.03 MPa	1.38 MPa	2.07 MPa
Channel 1	15.6	17.1	20.6	43
Channel 2	11.5	21.3	23.8	38.2
Channel 3	6.8	10.4	12.4	22.6
Channel 4	6.9	9.2	9.3	33.3
Channel 5	16.2	14.0	24.8	40.4
Channel 6	12.0	13.0	18.8	34.9
Channel 7	7.1	16.7	25.6	43.5
Channel 8	14.9	20.0	26.6	45.2

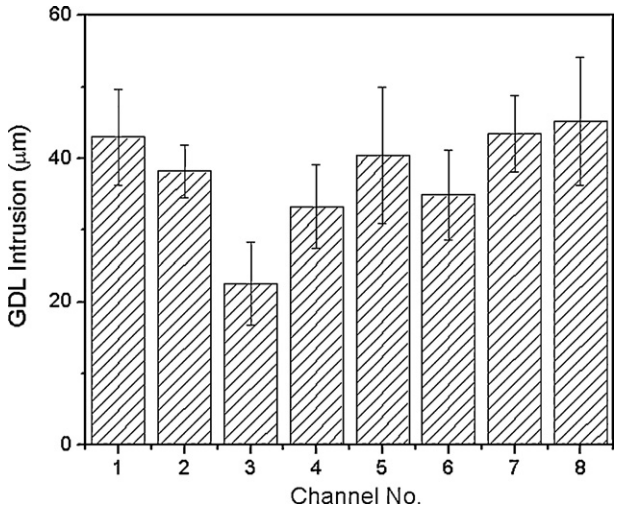

Fig. 8. Average GDL intrusions measured optically in the central region of gas channels.

icant local variation in structure. Some of these specific structural features are shown in Fig. 9. It should be noted that only the top surface of the GDL is focused in these images. As seen from Fig. 9(a) and (b), the fiber arrangement (that is the number of fibers in a unit area) on the top surface of the GDL is not uniform, but rather divergent between the sparse regions (Fig. 9(a)) and the dense regions (Fig. 9(b)). The size of these regions is estimated to be on the order of 1 mm, which is comparable to the channel width (0.7 mm) tested in this work. The sparse regions would have a higher tendency to deform under compression than the dense regions, leading to a variation of local GDL intrusion. A special region where numerous fiber ends aggregate is also observed and is shown in Fig. 9(c). It is expected that this part would have a large deformation if a channel is located in this region due to the termination of multiple fibers. There may be other variations in the GDL material, such as different distribution of binder materials, major fiber directions coinciding with the channel direction, etc., that contribute to the local mechanical deformation under compression.

By considering the relatively small area (active area of 18.2 cm^2) of the GDL tested in this work, the finding of the uneven intrusion has a profound impact on a PEMFC stack, which generally has a much larger active area and may contain tens to hundreds of such cells. Since GDL intrusion inevitably reduces the designed channel cross-sectional areas, flow maldistribution inevitably results. Even worse, the liquid water holdup in the intruded channels will increase and is difficult to remove because the intruded channels feature a greater flow resistance and hence a lower gas velocity. The presence of more liquid water further increases the flow resistance and reduces the gas flow through the channel. This feedback mechanism further worsens the channel flooding.

3.2. Flow distribution measurement

A direct result of the uneven GDL intrusion in gas channels is the flow maldistribution, which has a significant impact on fuel cell performance and durability. Therefore, it is of critical importance to experimentally investigate the flow distribution in PEMFC gas channels. For this purpose, the flow rate in an individual channel is measured with the entrance region pressure drop method [25,26]. Fig. 10 shows the flow distribution for three total input flow rates, 1000, 2000 and 3000 sccm, at a compression of 2.07 MPa. The average channel flow rates are shown as dashed lines in Fig. 10. It is seen from Fig. 10 that channels 7 and 8 consistently have the lowest flow rates, and channels 3, 4 and 6 have higher flow rates. This flow maldistribution is believed to result from the uneven GDL intrusion. Two main causes for the uneven GDL intrusion have been established in the above section. One is the uneven distribution of the compression pressure caused by the tightening bolts. This may result in larger intrusion in the edge channels and consequently lower flow rate in these channels, exemplified by channel 8 in Fig. 10. Secondly, the flow maldistribution in the central channels (channel 2–7) may be due to the local variation of the GDL material.

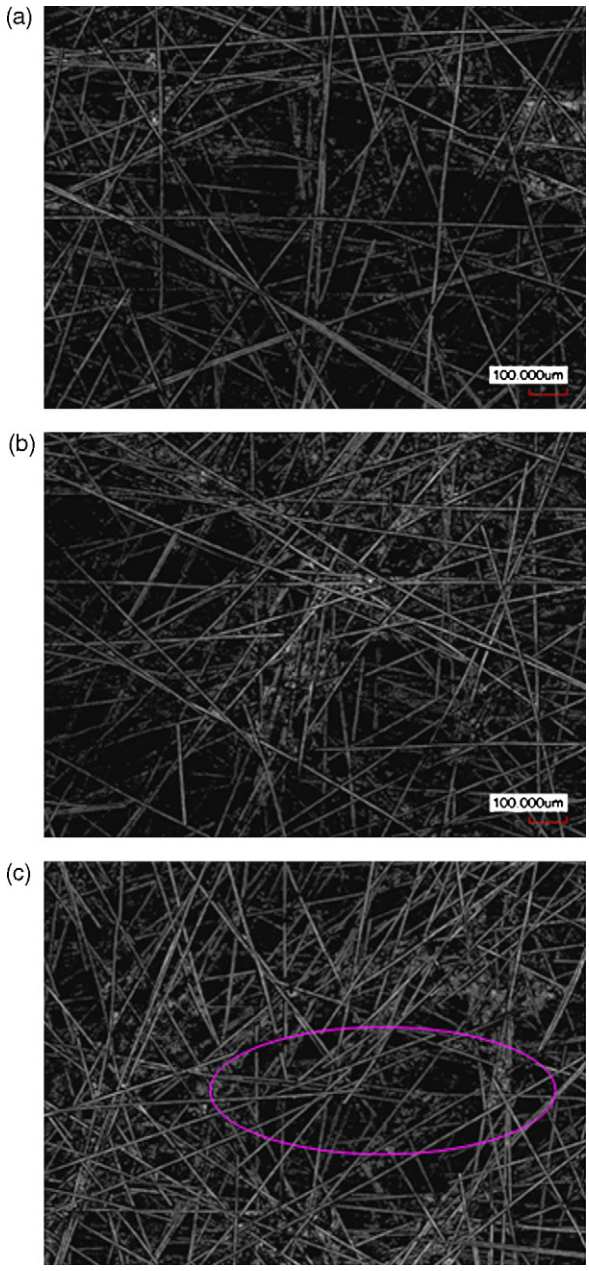

Fig. 9. Confocal microscope images of GDL top surface showing different structural features: (a) sparse fiber arrangement, (b) dense fiber arrangement and (c) aggregation of fiber ends.

It is not possible to relate the flow distribution measurements in Fig. 10 directly to the GDL intrusion measurements in Figs. 5 and 8 because there is no optical access into the test section for the intrusion measurements. Further, the intrusion data in Figs. 5 and 8 are optically measured only in a few locations, while the flow rate maldistribution is an overall result across the entire channel length. However, the correlation between the flow maldistribution and the uneven GDL intrusion is clear from these figures. In order to further

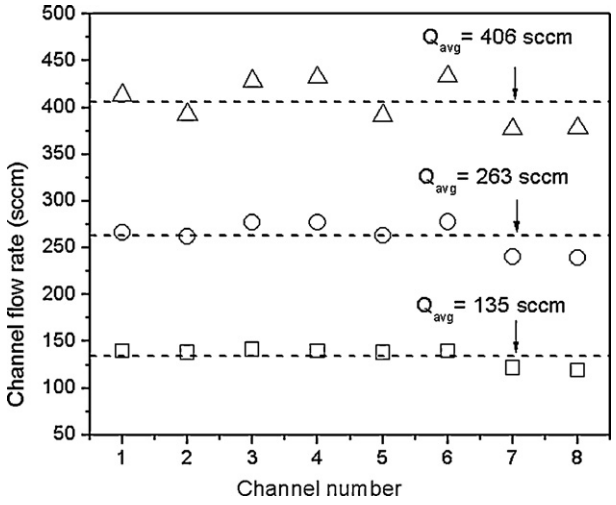

Fig. 10. Flow maldistribution obtained from flow measurement for three total input flow rates: 1000 sccm (symbol □), 2000 sccm (symbol ○) and 3000 sccm (symbol Δ). The compression used for the flow experiment is 2.07 MPa. The dashed lines show the average flow rate for each case.

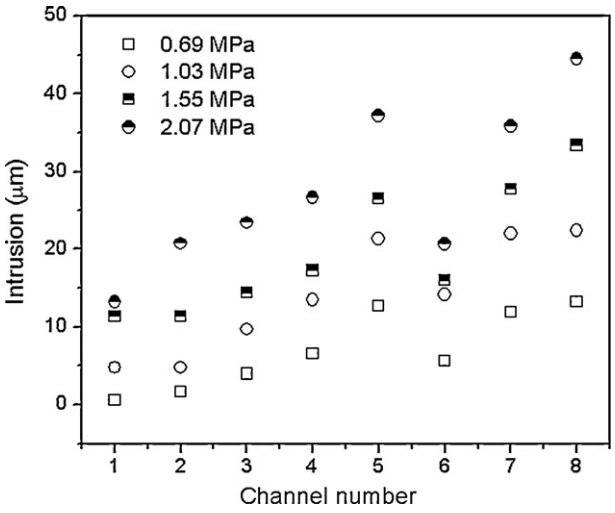

Fig. 11. The equivalent GDL intrusion calculated from a fluid flow model using the measured flow rates in each channel.

investigate the relationship between them, the equivalent intrusion is calculated from the data of measured flow rates and the pressure drop over the entire channel length based on conventional fluid mechanics theory (considering the entrance region effects).

From the fluid mechanics model, the measured flow rate can provide an estimate of channel intrusion and intrusion variation, and vice versa. A similar procedure has been used by Lai et al. [22]. In their work, a fully developed laminar Haggen–Poiseuille flow is assumed in gas channels without considering minor losses. However, for a fuel cell gas channel the pressure drop from the inlet to the outlet has the combined contributions from the bending, cross-sectional area changes, and entrance and exit losses. Without considering the minor losses, the measurements are believed to cause significant errors in the estimation of GDL intrusion. For this purpose, both the core and minor pressure drops are taken into account in this work. The core pressure drop p_{core} is calculated as follows [28]

$$\Delta p_{core} = 2\frac{f_{app}\ Re\, u\mu x}{D_h^2} \tag{1}$$

where f_{app} accounts for the pressure drop due to friction and the developing region effects. Its value is obtained based on conventional correlations [29]. Re, u, μ, D_h and x are the Reynolds number, fluid velocity and fluid viscosity, hydraulic diameter and channel length, respectively. D_h is defined as:

$$D_h = \frac{4A_c}{P_w} = \frac{4WH}{2(W+H)} \tag{2}$$

where A_c, P_w, W and H are the cross-sectional area, wetted perimeter, channel width and channel height, respectively.

Minor losses are difficult to predict, while the core pressure drop can be predicted well by conventional correlations. To estimate the minor loss, the pressure drop measurements using a plastic sheet as channel base are first carried out. The hardness of the plastic is high enough to be viewed as a rigid surface. No intrusion was observed for the plastic film with the optical measurement. The channel hydraulic diameter can thus be obtained accurately. Hence, it is possible to estimate the core pressure drop accurately based on the flow rate and hydraulic diameter. Then the minor pressure drop Δp_{minor} is obtained as follows:

$$\Delta p_{\min or} = \Delta p_{plast,meas} - \Delta p_{plast,core} \tag{3}$$

where $\Delta p_{plast,meas}$ and $\Delta p_{plast,core}$ are the total and core pressure drops with plastic sheet. Once the minor pressure loss is determined, the core pressure drop with GDL intrusion can be calculated as:

$$\Delta p_{GDL,core} = \Delta p_{GDL,meas} - \Delta p_{\min or} \tag{4}$$

where $\Delta p_{GDL,meas}$ is the total pressure drop of GDL measured by a flow meter. It is assumed that the minor losses would remain same, which is not entirely correct, but is able to provide a reasonable estimate of the GDL core pressure drop. Using the calculated core pressure drop, the actual channel hydraulic diameter is estimated using Eq. (1). The channel height then can be obtained from the following equation:

$$H = \frac{WD_h}{2W - D_h} \tag{5}$$

The equivalent intrusion is defined as the difference between the designed channel height (0.4 mm) and the calculated channel height H. The equivalent GDL intrusions for all the channels at different compressions are shown in Fig. 11. An uneven intrusion from channel to channel is again observed in this plot.

3.3. Pressure drop in gas channels

Fig. 12 shows a comparison of experimental measurements and predicted pressure drops as a function of total air flow rate. The plastic sheet results represent non-intruded channels and thus yield the lowest pressure drop for a given flow rate. The actual GDL measurements yield a higher value of pressure drop over the entire flow rate range. The three lines represent the results from the simulation with three values of intrusion, which was assumed to be uniform. It is seen that the GDL data matches closely within 10% with the intrusion simulation results except for the highest flow rate case. For the highest flow rate of 3000 sccm, the GDL data fall on the 20% intrusion line. This indicates that it may not be appropriate to consider the intrusion to be uniform throughout the channel, but may act as a series of orifices whose characteristics may not be represented by a simple uniform intrusion model.

Fig. 13 shows the results of simulation depicting the effects of GDL intrusion on pressure drop and flow rate. The results are calculated for the same test section having eight channels with the following dimensions: 0.7 mm (width) × 0.4 mm (height) × 183 mm (length). As seen from this figure, the pressure drop increases non-linearly with intrusion for a given flow rate. For

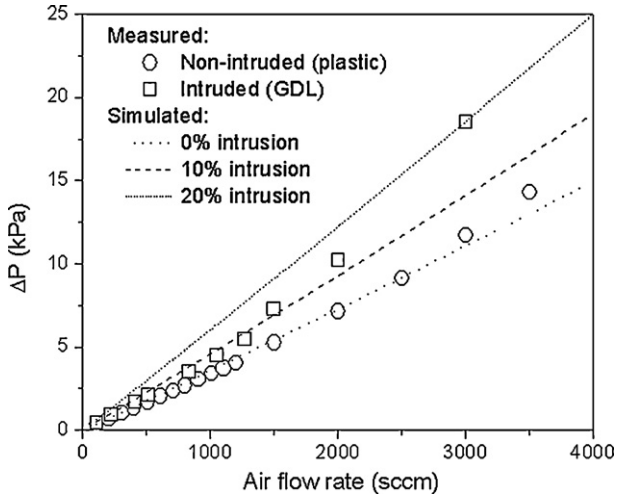

Fig. 12. Total pressure drop for the cases of intruded channels (with GDL) and non-intruded channels (with plastic sheet) as a function of air flow rate. The test section is compressed to 2.07 MPa. The lines show the results from fluid flow model without intrusion and with 10% and 20% intrusion.

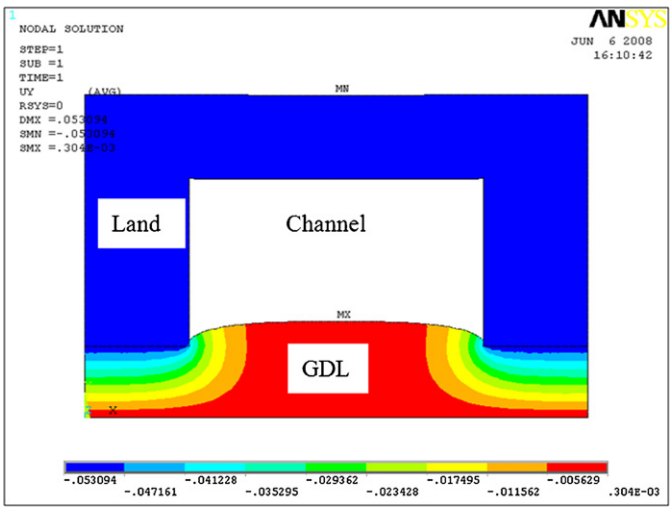

Fig. 14. ANSYS nodal solution for GDL displacement at compression of 2.07 MPa.

example, an intrusion of 20% will approximately double the pressure drop, from 3.6 kPa without intrusion to 6.1 kPa with intrusion. Likewise, intrusion in a channel will drastically decreases the flow rate in the channel for a given total pressure drop. A 10% intrusion will lead to a decrease in the flow rate from 1000 to 780 sccm, which is more than 20% reduction. Due to its profound impact on pressure drop and flow rate distribution, the GDL intrusion must be considered in PEMFC design, as it is inevitable during assembly of PEMFCs.

3.4. Determination of elastic modulus of GDL

ANSYS was used to simulate the deformation of the GDL under the lands. Fig. 14 shows an example of ANSYS nodal solution of the displacement at a compression of 2.07 MPa. The displacement is measured vertically in millimeters, opposite the direction of the compressive force. The color (grayscale) gradient on the figure depicts the amount of displacement seen by the channel plate and the GDL, with red (light) indicating little displacement and blue (dark) indicating the most displacement. The model shows that there is little displacement (0.3 μm) at the center of the GDL surface in the channel, while the GDL under the land region experiences significant compression. This analysis shows that intrusion is the apparent rise of the GDL surface into the gas channels. However, the cause of the intrusion is the displacement of the lands compressing the GDL under it, with no direct compression at the center of the channel.

Comparisons of the GDL intrusion obtained from the optical measurements and the fluid flow analysis are shown in Fig. 15. The intrusions in this figure are the average intrusion from all 8 channels. The equivalent intrusion is also obtained by the finite element (ANSYS) simulation varying Young's modulus. When a Young's modulus of 17.9 MPa, which is estimated for Toray paper [5], is used, the ANSYS simulation gives much higher intrusion values as shown in Fig. 15. Instead, a Young's modulus of 30.94 MPa shows a good agreement with optical measurements and fluid mechanics calculation. This difference in Young's modulus may be due to the differences in the fiber samples or may reflect the effect of the MPL. Further characterization of the MPL is recommended for future work.

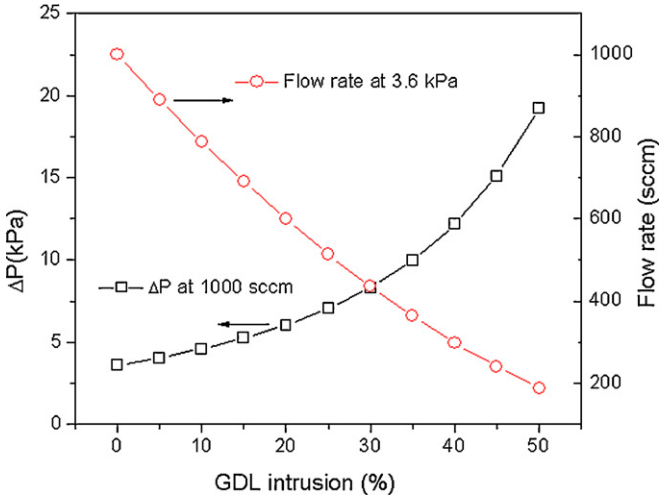

Fig. 13. Simulation results showing the effects of GDL intrusion on: (i) the total pressure drop at a given flow rate of 1000 sccm, and (ii) the channel flow rate at a given pressure drop of 3.6 kPa.

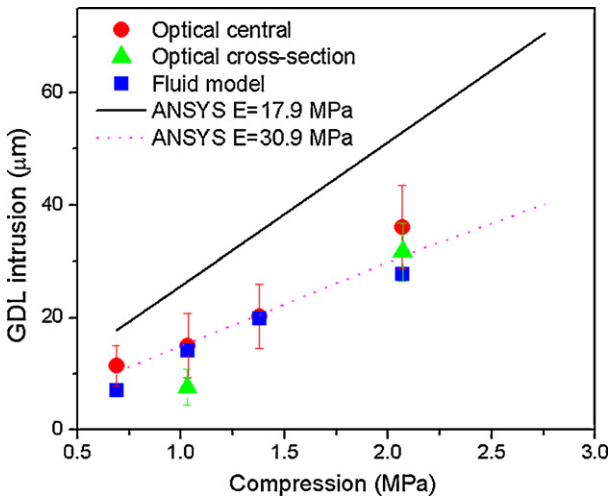

Fig. 15. Comparison of intrusion from fluid flow model and ANSYS simulation results.

4. Conclusions

The GDL intrusion into gas channels of a PEMFC under different compressions is investigated by optical measurements, a fluid mechanics model, and a finite element analysis (ANSYS) simulation. Optical measurements are carried out in the cross-section and the central regions of the channels using a confocal microscope. The measurements from the optical measurements and the fluid mechanics model are in good agreement with each other. As expected, the intrusion increases with increasing compression. A hysteresis in intrusion is found when cycling from increasing to decreasing compression. The most important finding is the uneven distribution of GDL intrusion into the gas channels. The heterogeneous GDL structure is assumed to be partially responsible for the non-uniform intrusion, while the uneven clamping force distribution may also lead to higher intrusion in the edge channels.

A direct consequence of the uneven GDL intrusion is the flow maldistribution, which is verified by the flow distribution measurements in individual channels. A specially designed test section is used to obtain the flow rate in the individual channels. The reduced channel hydraulic diameter is then calculated with a refined fluid mechanics model based on the flow rate measurements. The minor losses in the flow developing region are accounted for to allow for a more accurate calculation of GDL intrusion. The equivalent intrusion derived from the fluid mechanics model is comparable to the optical measurements. An uneven distribution of GDL intrusion is again observed. The pressure drop along the gas channel from the experimental measurements is compared with the prediction. It is found that the GDL intrusion must be accounted for in order to have a good estimation of the total pressure drop. The average intrusion is estimated to be around 10% for the GDL case, while the plastic sheet shows essentially no intrusion. The uniform intrusion model is able to represent the channel flow characteristics reasonably well, except at high flow rates. A model using multiple orifices in series is suggested to accurately depict the intrusion effect on the flow.

The numerical ANSYS simulation provides a way to estimate the mechanical properties of a GDL by using the measured values of intrusion. The Young's modulus of the investigated GDL is estimated to be 30.94 MPa, which is larger than that of the Toray carbon paper with a reported value of 17.9 MPa. This difference is considered to be due to the different materials and the presence of MPL.

Acknowledgements

This work was conducted under the project entitled "Visualization of Fuel Cell Water Transport and Performance Characterization under Freezing Conditions" sponsored by US Department of Energy grant DE-FG36-07GO17018. The collaborative efforts of Dr. Thomas Trabold and Mr. Jon Owejan at the General Motors Fuel Cell Research Center at Honeoye Falls, NY, are gratefully acknowledged.

References

[1] K. Miyatake, M. Watanabe, J. Mater. Chem. 16 (2006) 4465–4467.
[2] B. Smitha, S. Sridhar, A.A. Khan, J. Membr. Sci. 259 (2005) 10–26.
[3] H.A. Gasteiger, S.S. Kocha, B. Sompalli, F.T. Wagner, Appl. Catal. B: Environ. 56 (2005) 9–35.
[4] Y. Shao, J. Liu, Y. Wang, Y. Lin, J. Mater. Chem. 19 (2009) 46–59.
[5] M. Mathias, J. Roth, J. Fleming, W. Lehnert, in: W. Vielstich, H. Gasteiger, A. Lamm (Eds.), Handbook of Fuel Cells—Fundamentals, Technology and Applications, vol. 3, John Wiley & Sons Ltd., 2003.
[6] Z. Qi, A. Kaufman, J. Power Sources 109 (2002) 38–46.
[7] U. Pasaogullari, C.Y. Wang, K.S. Chen, J. Electrochem. Soc. 152 (2005) A1574–A1582.
[8] X. Wang, J. Zhang, H. Xu, X. Zhu, J. Chen, B. Yi, J. Power Sources 162 (2006) 474–479.
[9] L.R. Jordan, A.K. Skukla, T. Behrsing, N.R. Avery, B.C. Muddle, M. Forsyth, J. Appl. Electrochem. 30 (2000) 641–646.
[10] C.S. Kong, D.Y. Kim, H.K. Lee, Y.G. Shul, T.H. Lee, J. Power Sources 108 (2002) 185–191.
[11] J.P. Owejan, J.E. Owejan, T.W. Tighe, W. Gu, M. Mathias, Proceedings of Fluids Engineering Division Summer Meeting 2007, 5th Joint ASME/JSME Fluids Engineering Conference, San Diego, CA, USA, July 30–August 2, 2007.
[12] W. Lee, C.H. Ho, J.W.V. Zee, M. Murthy, J. Power Sources 84 (1999) 45–51.
[13] J. Ge, A. Higier, H. Liu, J. Power Sources 159 (2006) 922–927.
[14] S. Escribano, J.F. Blachot, J. Etheve, A. Morin, R. Mosdale, J. Power Sources 156 (2006) 8–13.
[15] P. Zhou, C.W. Wu, J. Power Sources 170 (2007) 93–100.
[16] I. Nitta, O. Himanen, M. Mikkola, J. Power Sources 171 (2007) 26–36.
[17] I. Nitta, O. Himanen, M. Mikkola, Electrochem. Commun. 10 (2008) 47–51.
[18] J.P. Feser, A.K. Prasad, S.G. Advani, J. Power Sources 162 (2006) 1226–1231.
[19] A. Bazylak, D. Sinton, Z.S. Liu, N. Ajilali, J. Power Sources 163 (2007) 784–792.
[20] T. Hottinen, O. Himanen, Electrochem. Commun. 9 (2007) 1047–1052.
[21] T. Hottinen, O. Himanen, S. Karvonen, I. Nitta, J. Power Sources 171 (2007) 113–121.
[22] Y.H. Lai, P.A. Rapaport, C. Ji, V. Kumar, J. Power Sources 184 (2008) 120–128.
[23] S. Basu, J. Li, C.-Y. Wang, J. Power Sources 187 (2009) 431–443.
[24] J.P. Owejan, J.J. Gagliardo, J.M. Sergi, T.A. Trabold, S.G. Kandlikar, Int. J. Hydrogen Energy 34 (2009) 3436–3444.
[25] Z. Lu, S.G. Kandlikar, C. Rath, M. Grimm, W. Domigan, A.D. White, M. Hardbarger, J.P. Owejan, T.A. Trabold, Int. J. Hydrogen Energy 34 (2009) 3445–3456.
[26] S.G. Kandlikar, Z. Lu, W.E. Domigan, A.D. White, M.W. Benedict, Int. J. Heat Mass Transf. 52 (2009) 1741–1752.
[27] L.K. Saha, E. Kurihara, W. Shi, N. Oshima, Proceedings of the International Conference on Nanochannels, Microchannels, and Minichannels ICNMM2008-62211, 2008.
[28] S.G. Kandlikar, S. Garimella, D. Li, S. Colin, M.R. King, Heat Transfer and Fluid Flow in Minichannels and Microchannels, Elsevier, 2006.
[29] R.J. Philips. M.S. Thesis, Department of Mechanical Engineering, Massachusetts Institute of Technology, Cambridge, MA, 1987.